Deposition of hydroxyapatite on SiC nanotubes in simulated body fluid

Tomitsugu Taguchi[a], Toshiki Miyazaki[b], Satoshi Iikubo[b], Kenji Yamaguchi[a]

[a] Quantum Beam Science Directorate, Japan Atomic Energy Agency, Tokai-mura, Ibaraki-ken 319-1195 Japan

[b] Graduate School of Life Science and Systems Engineering, Kyushu Institute of Technology, Wakamatsu-ku, Kitakyushu-shi, Fukuoka-ken 808-0196 Japan

Abstract

Hydroxyapatites were found to on SiC nanotubes treated with NaOH and subsequently HCl solution after soaking in simulated body fluid. On the other hand, hydroxyapatites did not deposit on as-received SiC nanotubes, the SiC nanotubes with NH_4OH solution treatment and SiC bulk materials with NaOH and subsequently HCl solution treatment. Therefore, we succeeded in the development of bioactive SiC nanotubes by downsizing SiC materials to nanometer size and treating with NaOH and subsequently HCl solutions for the first time.

Keywords

Silicon carbide, Nanotubes, Hydroxyapatite, Simulated body fluid

1. Introduction

Silicon carbide (SiC) is being developed as structural materials for gas turbines in aerospace planes and blanket components in fusion reactors due to its light weight and excellent mechanical properties [1-3]. The SiC nanotubes, which had tubular configures with outer diameters of approximately 100 nm, were successfully synthesized in our previous studies [4, 5]. Among one-dimensional nanomaterials, carbon nanotubes (CNTs) are well known and the most important materials for electrical, mechanical and medical applications [6-8]. In the medical field, particularly orthopedics, CNTs are expected to be using as reinforcements of various biomaterials [9]. Morisada et. al. has reported that the strength and fracture toughness of SiC material increased by dispersing with SiC layer coated multi-walled carbon nanotubes (MWNTs), while those did not increase by dispersing with as-received MWNTs [10]. Therefore, SiC nanotubes can become candidate reinforcement materials for dental and orthopedic implants in order to improve their mechanical properties such as strength and fracture toughness. Bioactive properties of SiC nanotubes are required to use them as reinforcement materials for biomaterials. So far, there have been a few reports about the deposition of hydroxyapatite on CNTs after soaking in simulated body fluid (SBF) [11, 12]. It has not

been, however, reported about the development of bioactive SiC materials.

Here, we report that hydroxyapatites deposited on SiC nanotubes with NaOH solution treatment after soaking in SBF. In other words, the bioactive SiC materials can be successfully developed for the first time in this study. Furthermore, the mechanism of hydroxyapatite formation on SiC nanotubes in SBF was discussed. The results and discussions in this study lead to a new suggestion of hydroxyapatite formation mechanism in SBF, affected dominantly by increase of specific surface area and existence of submicrometer-sized space due to downsizing of SiC materials.

2. Experimental

2.1 Sample preparation

Three kinds of SiC nanotubes without or with NaOH or NH_4OH solution treatment were prepared. SiC nanotubes were synthesized by the reaction of CNTs (as template materials) with Si powder at 1200 ºC in a vacuum for 100 h. Details of the fabrication process and characterization of SiC nanotubes are given elsewhere [4, 5]. SiC nanotubes were treated with 5M NaOH solution at 60 ºC for 24 h. The SiC nanotubes were removed from 5M NaOH solution, rinsed with ultrapure water, and then dried at room temperature. Subsequently, the SiC nanotubes after NaOH treatment were treated with 0.1M HCl solution at 40 ºC for 24 h. The SiC nanotubes were also removed from

HCl solution, rinsed with ultrapure water, and finally dried at room temperature. Another sample of SiC nanotubes were treated with 10M NH_4OH solution at 60 ºC for 24 h. The sample was removed from NH_4OH solution, rinsed with ultrapure water, and then dried at room temperature. In addition, chemical vapor deposited SiC (CVD-SiC, Toshiba Denko Co. Ltd., Japan) was also examined as bulk SiC materials.

2.2 Soaking in SBF

The hydroxyapatite formation ability of SiC nanotubes without or with alkali treatments was evaluated in SBF. The SiC nanotubes without and with two kinds of alkali treatment were then soaked for various periods in 100 ml of SBF with inorganic ion concentrations (Na^+ 142.0; K^+ 5.0; Mg^{2+} 1.5; Ca^{2+} 2.5; Cl^- 147.8; HCO_3^- 4.2; HPO_4^{2-} 1.0; and SO_4^{2-} 0.5 mol/m^3, pH 7.40) nearly equal to those of human blood plasma at 37.0 ºC [13]. The fluid was prepared by dissolving reagent-grade NaCl, $NaHCO_3$, KCl, $K_2HPO_4 \cdot 3H_2O$, $MgCl_2 \cdot 6H_2O$, $CaCl_2$ and Na_2SO_4 in ultrapure water and buffering at pH 7.40 with tris(hydroxymethl)aminomethane ($(CH_2OH)_3CNH_2$) and an appropriate amount of HCl aqueous solution. The samples were removed from SBF after a given period, rinsed with ultrapure water, and then dried at room temperature.

2.3 Characterization

The X-ray diffraction measurements were carried out at 30 kV and 20 mA using Cu-Kα radiation with a step-scanning technique in θ-2θ mode. Microstrucutural observations were conducted using a scanning electron microscope (SEM, Model JSM-T220A, JEOL Ltd., Tokyo, Japan) operated at 30 kV and a transmission electron microscope (TEM, Model 2000F, JEOL Ltd., Tokyo, Japan) operated at 200 kV. A holey-carbon copper grid sample holder was used for TEM observations. Energy dispersive X-ray spectroscopy (EDS, Model Noran 623M-3SUT, Thermo Electron Corporation, Yokohama, Japan) analysis was also carried out in order to evaluate the chemical composition of the samples. The chemical bonding states of the samples were determined using X-ray photoelectron spectroscopy (XPS, Model KRATOS AXIS-His, Shimadzu Co, Japan). The zeta potential analyzer (Model ELS-Z Otsuka Electronics Co.,Ltd., Japan) was used to measure the zeta potential of the samples.

3. Results

Figure 1 (a) shows the X-ray diffraction patterns of SiC nanotubes without or with NH_4OH or NaOH treatment after soaking in SBF for 14 days. The peak of hydroxyapatite was observed in the SiC nanotubes with NaOH treatment after soaking

in SBF, while it was not observed in the SiC nanotubes with NH_4OH treatment and without alkali treatment. The X-ray diffraction patterns of SiC nanotubes with NaOH treatment after soaking in SBF for 0, 1, 4, 7 and 14 days are also given in Fig. 1 (b). These results reveal that the broad peak of hydroxyapatite around 32º began to be observed in SiC nanotubes with NaOH treatment after soaking for 1 day, and its intensity increased with increasing the soaking time in SBF. The peak of X-ray diffraction patterns around 32º in the SiC nanotubes with NaOH treatment after soaking for 1 day seemed to be different from those after soaking for more than 4 days. The peak in the SiC nanotubes after soaking for 1 day had sharper configuration compared to those after soaking for more than 4 days. The sharp peak around 31º overlapped the broad peak of hydroxyapatite around 32º in the SiC nanotubes after soaking for 1 day. The sharp peaks around 31º and 45º were indexed to NaCl, attributing to SBF [14]. On the other hand, the peaks indexed to NaCl crystal were not observed in the SiC nanotubes with NaOH treatment after soaking for more than 4 days. Since the amount of deposited hydroxyapatite increased with increasing the soaking time in SBF, the formation of NaCl by the evaporation of SBF on the SiC nanotubes might be inhibited.

Figure 2 shows the SEM images of SiC nanotubes without or with alkali treatment before and after soaking in SBF. No change was observed in SiC nanotubes without and

with NH_4OH treatment even after soaking in SBF for 14 days. According to SEM images, spherical grains began to be produced on SiC nanotubes with NaOH treatment after soaking in SBF for 1 day. The grain size and number of spherical grains were increased with increasing the soaking time in SBF. These results were consistent with the results of X-ray diffraction patterns.

Figure 3 shows the TEM images of as-received SiC nanotubes after soaking in SBF for 14 days and SiC nanotubes with NaOH treatment before and after soaking in SBF for 1 and 14 days. The TEM observations indicate that the spherical grains were formed on SiC nanotubes and their size increased with increasing the soaking time in SBF as well as SEM observation. On the other hand, the spherical grains were not observed on as-received SiC nanotubes even after soaking for 14 days. The spherical grains were consisted of many ultra-thin nanosheets. The thickness of ultra-thin nanosheets was approximately 5 nm. Therefore, the specific surface area of spherical grains may be very large compared to those of bulk materials. The nanosheets were crystalline. The EDS spectra of SiC nanotubes and spherical grains are given in Fig. 4. According to the EDS evaluations, the ultra-thin nanosheets were consisted of mainly Ca, P and O. These results and X-ray diffraction patterns reveal that the ultra-thin nanosheets were hydroxyapatites.

The electron diffraction pattern of hydroxyapatite on the SiC nanotubes with NaOH treatment after soaking for 1 day exhibited ring patterns, while that after soaking for 14 days showed some bright spots, as shown in Fig. 3 (d) and (e) insets. According to the electron diffraction patterns, the crystallinity of hydroxyapatite increased with increasing the soaking time.

Hydroxyapatites were successfully deposited on SiC nanotubes treated with NaOH and subsequently HCl solution by soaking in SBF for the first time. In other words, the bioactive SiC materials could be successfully developed for the first time in this study. Utilizing for the characterization of powdery configuration of SiC nanotubes, hydroxyapatites can be deposited on the selected surfaces of bioinert materials after soaking in SBF by selective coating with the bioactive SiC nanotubes. Moreover, the composites consisted of SiC and hydroxyapatite have a possibility of being used for various engineering applications such as structural materials composed of SiC nanotubes and hydroxyapatites, and a gas sensor of SiC nanotubes with hydroxyapatite phases as an adsorption material [10, 15, 16].

4. Discussion

Leonor et. al. reported that the mechanism of hydroxyapatite formation on

polyethylene modified with sulfonic groups in SBF was due to electrostatic interaction of the polymer surface and ions in the fluid [17]. In order to discuss the mechanism of the hydroxyapatite formation on SiC nanotubes treated with NaOH, the zeta potentials of SiC nanotubes without or with two kinds of alkali treatments were evaluated. Table I shows the variation of zeta potential of the surface of SiC nanotubes without or with alkali treatments. These results indicate that the zeta potential of SiC nanotubes changed to negative from positive by each alkali treatment. The zeta potential of SiC nanotubes with NH_4OH treatment was negative as well as that with NaOH treatment. Because hydroxyapatites didn't produce on the SiC nanotubes with NH_4OH treatment, the dominant reason of hydroxyapatite formation isn't the electrostatic interaction of nanotube surface and ions present in the SBF solution.

It has been reported about the mechanism of hydroxyapatite formation on silica induced by silanol groups [18-20]. The Si 2p core-level XPS spectra of SiC nanotubes without or with alkali treatment are shown in Fig. 5. As shown in the figure, the peak corresponding to Si-C bonds with the binding energy of 100.6 eV was clearly dominant, while the peaks of corresponding to $Si\text{-}O_2$ and Si-OH with the binding energies of 103.4 and 104.3 eV were slightly observed [21, 22]. These results reveal that ultrathin SiO_2 layer existed on the surface of SiC nanotubes and, in addition, slight amount of silanol

groups also existed on the surface of SiO_2 layer. Table II shows the various peak area fractions of Si-C, Si-O_2 and Si-OH peaks evaluated from the Si 2p XPS spectra of SiC nanotubes without or with two kinds of alkali treatments. The peak area fraction of Si-OH peak was smaller than 1 % before alkali treatment and almost constant after each alkali treatment. From above results, the existence of silanol groups on the surface of SiC nanotubes isn't also the dominant reason of hydroxyapatite formation in this study.

According to Si 2p XPS spectra, the peak area of Si-O_2 peak decreased by each alkali treatment. This result indicates the decrease and disappearance of thin SiO_2 layer from the surface of SiC nanotubes. Cho et. al. has reported that the adsorbed silicate ion to polyether sulfone substrate from silica gel is considered to be responsible for hydroxyapatite nucleation on the substrate [23]. The etching and/or damaging the thin SiO_2 layer by alkali treatments in this study might lead to the production of silicate ion. There is, therefore, a possibility that the silicate ion produced from thin SiO_2 layer caused the hydroxyapatite nucleation on the SiC nanotubes. In the previous studies, substrates were placed on silica materials with a distance of sub millimeter between them in SBF for a few days, and then soaked in a solution with ion concentrations 1.5 times those of SBF for roughly 1 week. After the second soaking, hydroxyapatites

formed on the substrates, whereas a small amount of hydroxyapatite nuclei are formed after the first soaking [23, 24]. In this study, hydroxyapatites formed on the SiC nanotubes even after soaking in SBF for 1 day. This result is not consistent in the previous studies. The specific surface area of SiC nanotubes was approximately 10 m^2/g evaluated by BET method. This value is much higher than that of bulk material. Many silicate ions enough to form hydroxyapatite nucleation might be produced from thin SiO_2 layer of SiC nanotube with NaOH treatment. It is, therefore, considered to be easy to form hydroxyapatites on SiC nanotubes with NaOH treatment. However, hydroxyapatites did not produce on SiC nanotubes with NH_4OH treatment, in spite of the decrease and disappearance of thin SiO_2 layer as well as the SiC nanotubes with NaOH treatment. Although the decrease and disappearance of thin SiO_2 layer occurred in the SiC nanotubes with NH_4OH treatment, silicate ions might not be produced by treated with NH_4OH solution. The further researches are required for the clarification of reason why hydroxyapatites did not produce on SiC nanotubes with NH_4OH treatment.

Figure 6 shows the SEM images of CVD-SiC with NaOH treatment before and after soaking in SBF. Hydroxyapatites were not observed on the surface of CVD-SiC with NaOH treatment even after soaking in SBF for 14 days, although they produced on SiC

nanotubes with NaOH treatment. The reason may be considered that enough many silicate ions to form hydroxyapatite nucleation were not able to produce from thin SiO_2 layer of CVD-SiC, because the specific surface area of CVD-SiC was much smaller than that of SiC nanotubes.

Sugino et. al. has reported about the formation of hydroxyapatites on the internal surfaces of the V-shaped titanium specimens established with a spatial gap by using the titanium wire after soaking in SBF, when the internal space height was approximately less than 600 μm [25]. It has been, furthermore, reported that a smaller gap established with titanium wire resulted in a large area of hydroxyapatites formation after soaking in SBF [25]. There was much submicrometer-sized space among the SiC nanotubes in this study. On the other hand, there was little space in CVD-SiC because it had smooth surfaces and a very low porosity. The silicate ions induced from thin SiO_2 layer might stagnate in the submicrometer-sized space among SiC nanotubes, and then the concentration of silicate ions might increase. Therefore, hydroxyapatites produced on the SiC nanotubes with NaOH treatment.

The mechanism of hydroxyapatites formation on the SiC nanotubes with NaOH treatment is very complicated (interaction of surfaces and ions in fluid, existence of silanol groups, amount and concentration of silicate ions and so on). Our study reveals

that the existence of submicrometer-sized space among the SiC nanotubes and increase of specific surface area of SiC nanotubes by downsizing of SiC materials may play important roles in depositing hydroxyapatite after soaking in SBF. The details of hydroxyapatite formation mechanism on SiC nanotubes have to be clarified by future work.

5. Conclusions

Three kinds of SiC nanotubes without or with NaOH or NH_4OH solution treatment were prepared and then soaked in SBF at 37.0 ºC for up to 14 days. In the result, hydroxyapatites deposited on SiC nanotubes treated with NaOH solution after soaking in SBF, while they did not deposit on as-received SiC nanotubes and the SiC nanotubes with NH_4OH treatment. In addition, they did not produce on the surface of SiC bulk materials with NaOH solution treatment. In other words, the bioactive SiC materials could be successfully developed for the first time by downsizing SiC materials to nanometer size and treating with NaOH solution. The hydroxyapatite formation mechanism on SiC nanotubes was also investigated. The results and discussions in this study lead to a new suggestion of hydroxyapatite formation mechanism in SBF, which is affected by not only conventional electrostatic interaction and the induced silanol

groups of the material surface but also increase of specific surface area and existence of submicrometer-sized space due to downsizing of SiC material.

Acknowledgment

This work was partly supported by a Grant-in-Aid for Young Scientists (B) (No. 23760646) from the Ministry of Education, Science, Sports and Culture of Japan.

Figure captions

Figure 1. X-ray diffraction patterns of (a) SiC nanotubes without or with NH_4OH or NaOH treatment after soaking in SBF for 14 days, and (b) SiC nanotubes with NaOH treatment after soaking in SBF for 0, 1, 4, 7 and 14 days.

Figure 2. SEM images of (a) as-received SiC nanotubes before soaking, (b) after soaking for 14 dyas, (c) SiC nanotubes with NH_4OH treatment after soaking for 14 days, (d) SiC nanotubes with NaOH treatment after soaking for 1 day, (e) 4 days and (f) 14 days.

Figure 3. TEM images of (a) low magnification and (b) high magnification of as-received SiC nanotubes after soaking for 14 days, (c) low magnification and (d) high magnification of SiC nanotubes with NaOH treatment after soaking for 1 day, (e) low magnification and (f) high magnification of SiC nantoubes with NaOH treatment after

soaking for 14 days.

Figure 4. EDS spectra of SiC nanotube and spherical grain in the SiC nanotubes with NaOH treatment after soaking for 14 days.

Figure 5. Si 2p core-level XPS spectra of (a) as-received SiC nanotubes, (b) SiC nanotubes with NH_4OH treatment, (c) SiC nanotubes with NaOH treatment before soaking in SBF.

Figure 6. SEM image of CVD-SiC with NaOH treatment (a) before and (b) after soaking in SBF for 14 days.

Tables

Table 1 Variation of zeta potential of the surface of SiC nanotubes without or with NH_4OH or NaOH treatments.

Kinds of specimens	Zeta potential / mV
As-received SiCNTs	32.5±1.8
SiCNTs treated with 10M NH_4OH	-34.1±0.1
SiCNTs treated with 5M NaOH and 0.2M HCl	-20.7±0.4

Table 2 Various peak area fractions of Si-C, Si-O-Si and Si-OH peaks evaluated from the

Si 2p XPS spectra of SiC nanotubes without or with NH_4OH or NaOH treatment.

Kinds of specimens	Si-C / %	$Si-O_2$ / %	Si-OH / %
As-received SiCNTs	96.0	3.4	0.6
SiCNTs treated with 10M NH_4OH	99.4	0.4	0.2
SiCNTs treated with 5M NaOH and 0.2M HCl	98.6	0.7	0.7

References

[1] T. Nozawa, T. Hinoki, A. Hasegawa, A. Kohyama Y. Katoh, L. L. Snead, C. H. Henager Jr., J. B. J. Hegeman, J. Nucl. Mater. 386-388 (2009) 622-627.

[2] C. H. Wei, P. F. Becher, J. Am. Ceram. Soc. 67 (1984) 571-574.

[3] Y. Akimune, T. Ogasawara, T. Akiba, N. Hirosaki, J. Mater. Sci. Lett. 10 (1991) 689-692.

[4] T. Taguchi, N. Igawa, H. Yamamoto, S. Jitsukawa, J. Am. Ceram. Soc. 88 (2005) 459-461.

[5] T. Taguchi, N. Igawa, H. Yamamoto, S. Shamoto, Physica E 28 (2005) 431-438.

[6] M. F. L. De Volder, S. H. Tawfick, R. H. Baughman, A. J. Hart, 339 (2013) 535-539.

[7] M. Scarselli, P. Castrucci, M. De Crescenzi, J. Phys. Condensed matter 24 (2012)

313202.

[8] L. P. Zanello, B. Zhao, H. Hu, R. C. Haddon, Nano letter 6 (2006) 562-567.

[9] S. Taruta, K. Kidokoro, T. Yamakami, T. Yamaguchi, K. Kitajima, M. Endo, N. Saito, J. Nanomaterials (2011) 935320.

[10] Y. Morisada, Y. Miyamoto, Y. Takaura, K. Hirota, N. Tamari, International Journal of Refractory Metals and Hard Materials 25 (2007) 322-327.

[11] T. Akasaka, F. Watari, Chem. Lett. 34 (2005) 826-827.

[12] S. Aryal, K. C. Remant Bahadur, N. Dharmaraj, K. W. Kim, H. Y. Kim, Scripta Materialia 54 (2006) 131-135.

[13] T. Kokubo, H. Kushitani, S. Sakka, T. Kitsugi, T. Yamamoto, J. Biomed. Mater. Res. 24 (1990) 721-734.

[14] D. H. Kwak, S. J. Hong, D. J. Kim, P. Greil, J. Ceram. Proc. Res. 11 (2010) 170-172.

[15] Y. B. Jia, G. L. Zhuang, J. G. Wang, J. Phys. D: Appl. Phys. 45 (2012) 065305.

[16] R. U. Mene, M. P. Mahabole, R. C. Aiyer, R. S. Khairnar, The Open Applied Physics Journal 3 (2010) 10-16.

[17] I. B. Leonor, H. M. Kim, F. Balas, M. Kawashita, R. L. Reis, T. Kokubo, T. Nakamura, J. Mater. Chem. 17 (2007) 4057-4063.

[18] H. Takadama, H. M. Kim, F. Miyaji, T. Kokubo, T. Nakamura, J. Ceram. Soc. Japan

108 (2000) 118-121.

[19] S. B. Cho, K. Nakanishi, T. Kokubo, N. Soga, J. Am. Ceram. Soc. 78 (1995) 1769-1774.

[20] S. B. Cho, F. Miyaji. T. Kokubo, K. Nakanishi, N. Soga, T. Nakamura, J. Mater. Sci. Med. 9 (1998) 279-284.

[21] Y. Hijikata, H. Yaguchi, M. Yoshikawa, S. Yoshida, Appl. Suf. Sci. 184 (2001) 161-166.

[22] J. H. Lee, Y. S. Kim, S. J. Kyung, J. T. Lim, G. Y. Yeon, J. Kor. Phys. Soc. 54 (2009) 981-985.

[23] S. B. Cho, F. Miyaji, T. Kokubo, K. Nakanishi, N. Soga, T. Nakamura, J. Biomed. Mater. Res. 32 (1996) 375-381.

[24] M. Tanahashi, T. Yao, T. Kokubo, M. Minoda, T. Miyamoto, T. Nakamura, T. Yamamoto, J. Am. Ceram. Soc. 77 (1994) 2805-2808.

[25] A. Sugino, K. Uetsuki, K. Tsuru, S. Hayakawa, A. Osaka, C. Ohtsuki, Mater. Trans. 49 (2008) 428-434.

Figure(s)

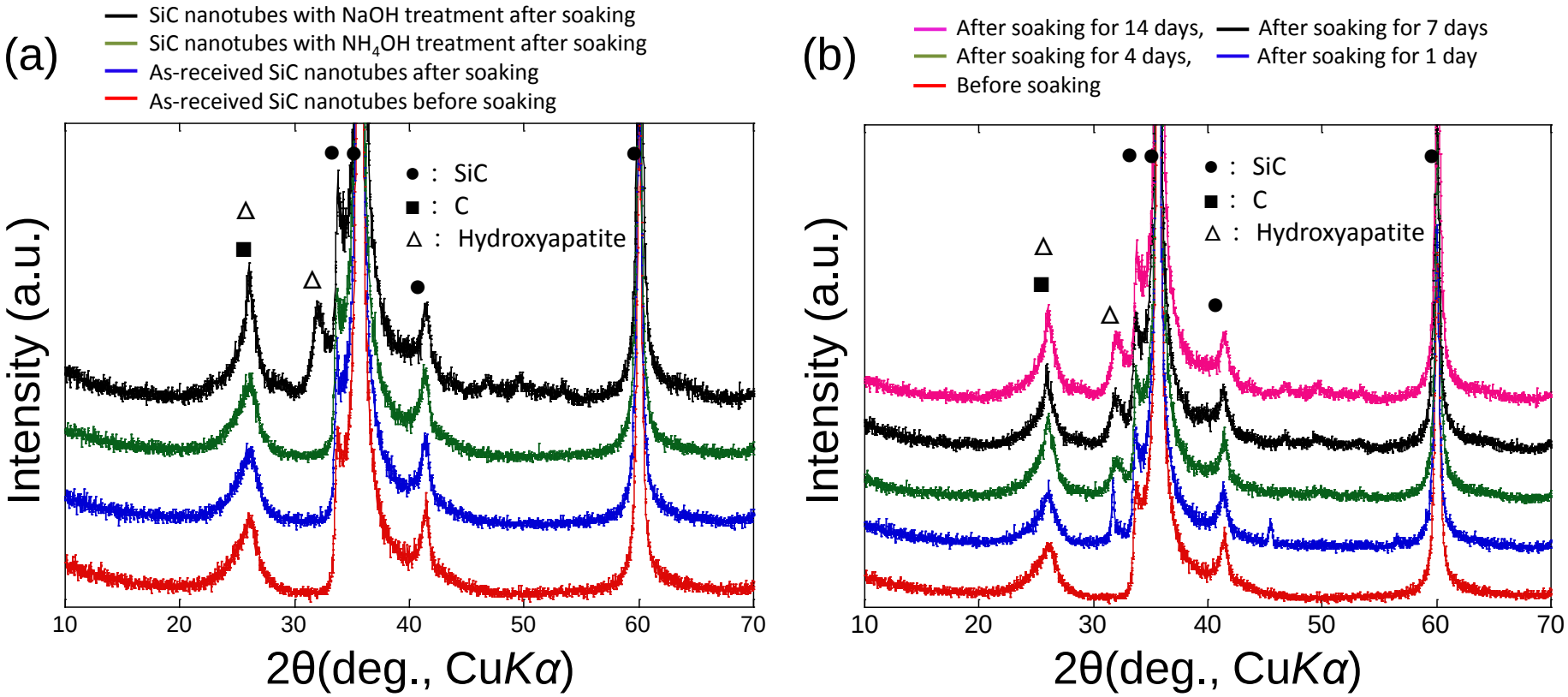

Figure 1

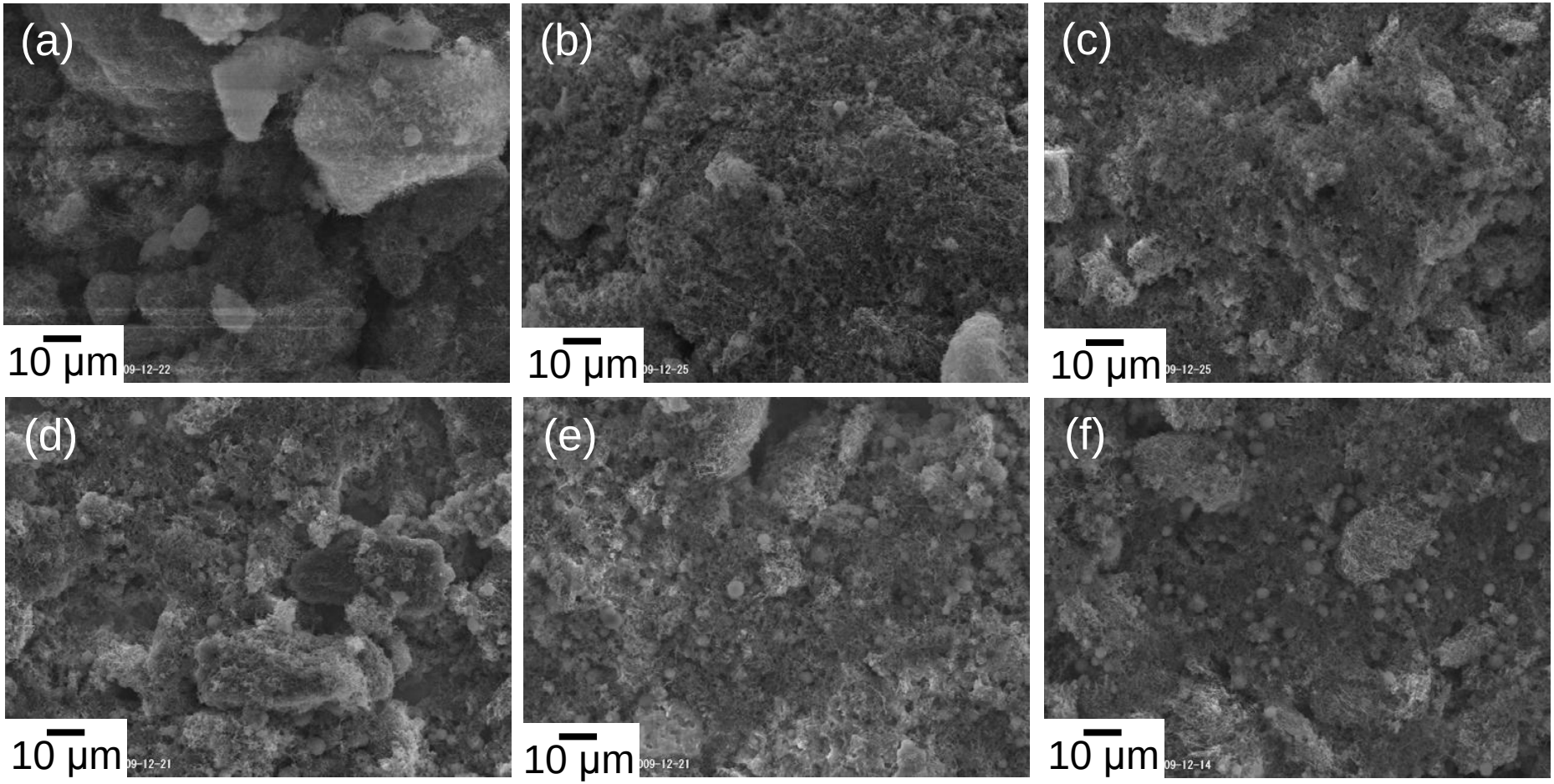

Figure 2

Figure 3

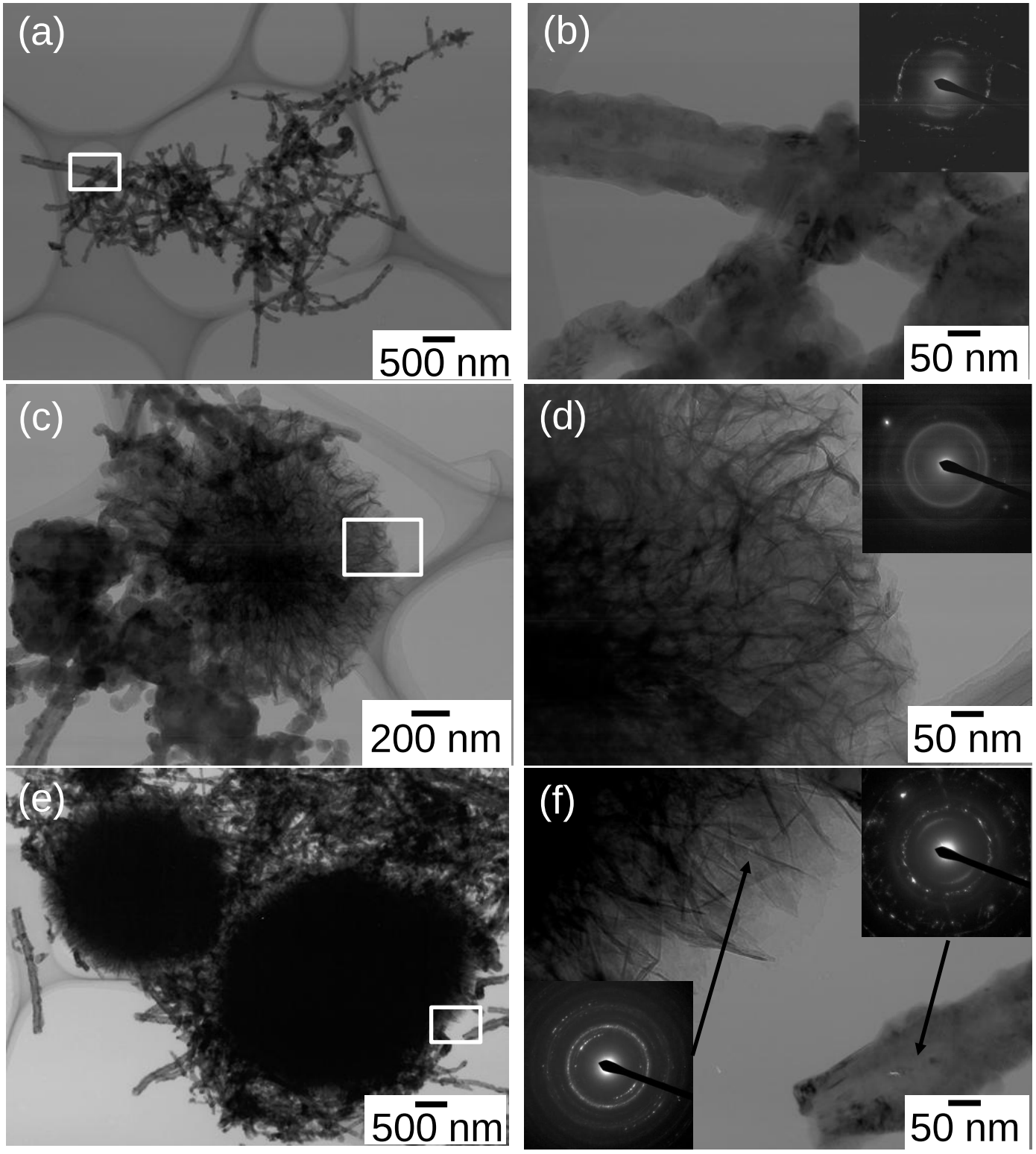

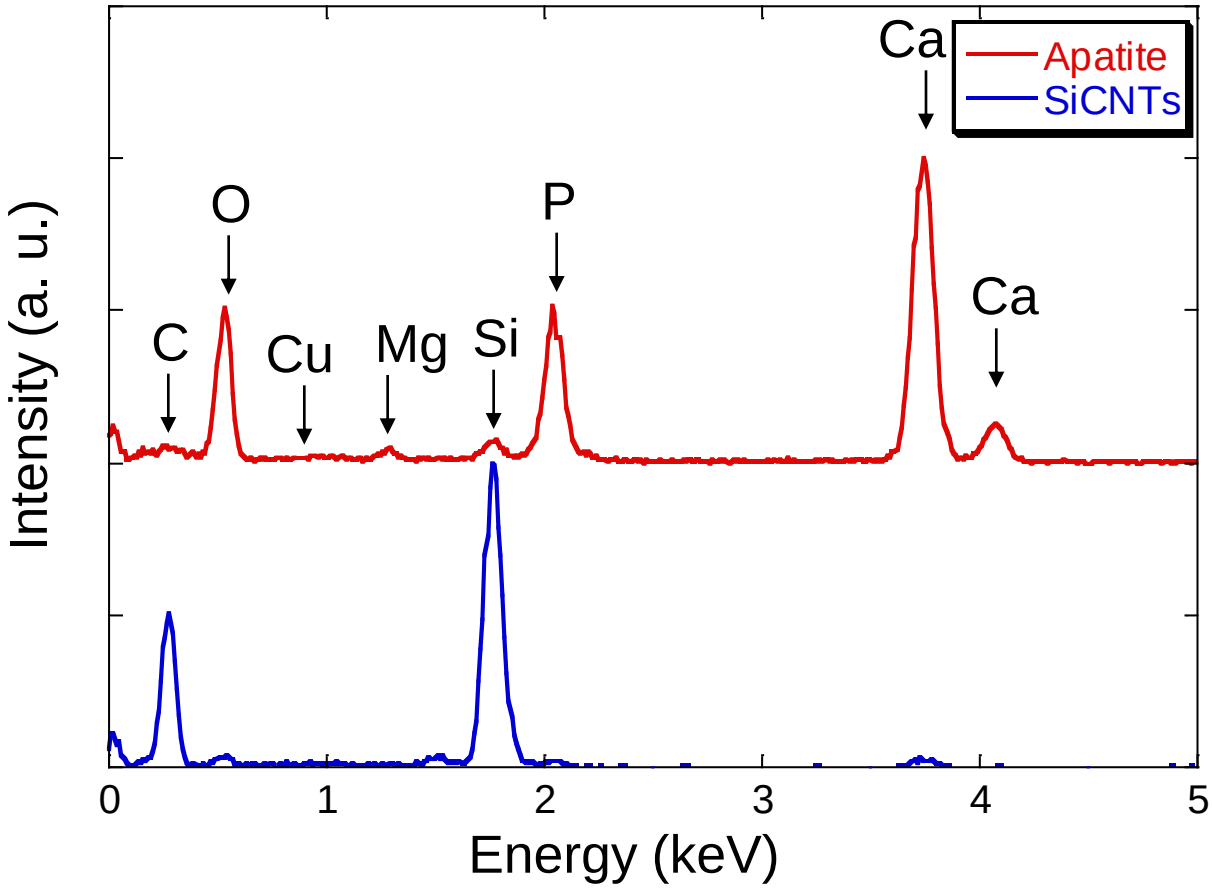
Ca
Apatite
SiCNTs
O
P
C
Cu
Mg
Si
Ca
Intensity (a. u.)
0
1
2
3
4
5
Energy (keV)

Figure 4

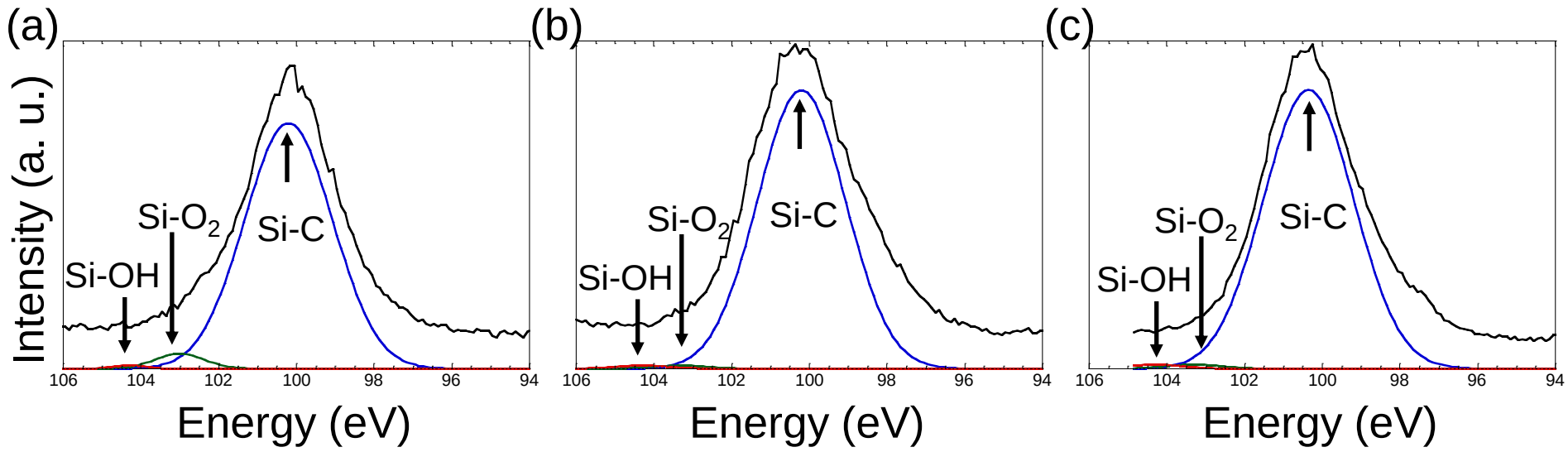
(a)
(b)
(c)
Intensity (a. u.)
Si-OH
Si-O2
Si-C
106
104
102
100
98
96
94
Energy (eV)

Figure 5

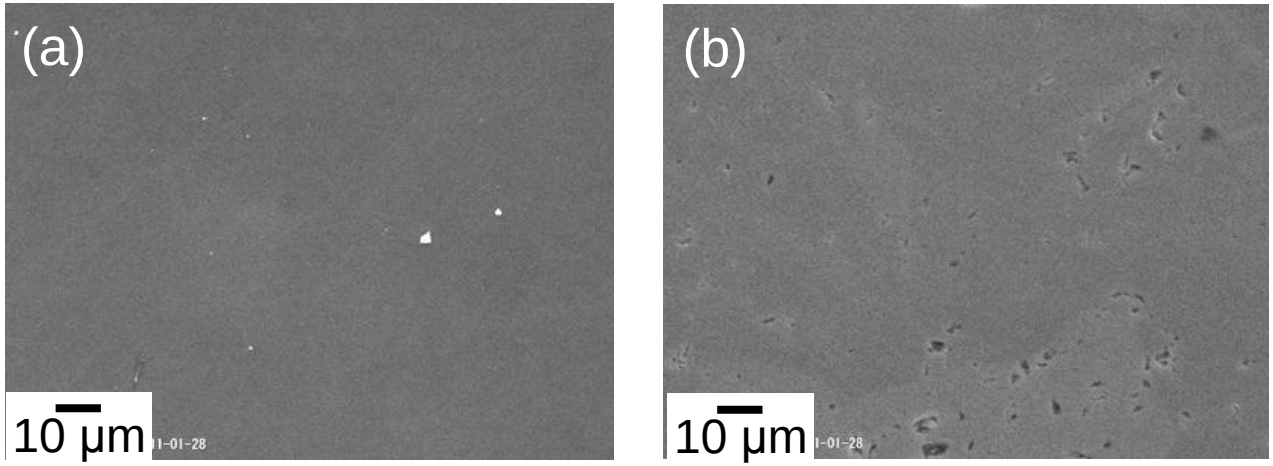

Figure 6